The Major Allergen from Birch Tree Pollen, Bet v 1, Binds and Permeabilizes Membranes†

Jesper E. Mogensen,‡,§ Mercedes Ferreras,|| Reinhard Wimmer,‡ Steen V. Petersen,⊥ Jan J. Enghild,⊥ and Daniel E. Otzen*,‡

Centre for Insoluble Protein Structures (inSPIN) at Department of Life Sciences, Aalborg University, Sohngaardsholmsvej 49, DK-9000 Aalborg, Denmark, Department of Molecular Biology, University of Aarhus, Gustav Wieds Vej 10C, DK-8000 Aarhus C, Denmark, and ALK-Abelló A/S, Bøge Alle 6-8, DK-2970 Hørsholm, Denmark

Received October 3, 2006; Revised Manuscript Received January 11, 2007

ABSTRACT: The 159 residue Bet v 1 is the major allergen from birch tree pollen. Its natural function is unknown although it is capable of binding several types of physiologically relevant ligands in a centrally placed cavity in the protein structure. Here we use circular dichroism and fluorescence spectroscopy to show that Bet v 1 binds to DOPC and DOPG phospholipid vesicles in a pH-dependent manner. Binding is facilitated by low pH, negatively charged phospholipids, and high vesicle curvature, indicating that electrostatic interactions and vesicle surface defects are important parameters for binding. Binding is accompanied by major structural rearrangements, involving an increase in α-helical structure and a decrease in β-structure. A bilayer structure per se is not a prerequisite for these rearrangements, since they also occur in the presence of the micelle-forming lysophospholipids lysoMPC and lysoMPG. Two major bound states (A and B) with distinct secondary structure compositions were identified, which predominate in the pH ranges ∼9.5−6.5 and ∼5−2.5, respectively. Despite the high content of secondary structure, the A- and B-states are partially unfolded as they unfold noncooperatively in CD thermal scans, in contrast to the native state. In addition, the B-state (but not the A-state) shows intermediate proteolysis-resistance and is able to induce complete leakage of calcein from the vesicles, indicating that this state is partially inserted into and significantly perturbs the bilayer structure. We conclude that Bet v 1 is a membrane binding protein, highlighting a possible biological function of this protein.

A major source of type I allergens in the temperate climate zone of the northern hemisphere is pollen from early flowering trees. More than 96% of patients allergic to tree pollen react toward Bet v 1[1] (*1*), which is the major allergen in birch trees (*2*). The protein consists of 159 amino acids and is constitutively expressed in birch tree pollen (*3*). Bet v 1 contains a seven stranded antiparallel β-sheet that wraps around a 25 residue long C-terminal α-helix (*4*). Bet v 1 has no dense hydrophobic core like typical globular proteins, but harbors a large forked cavity with three openings, allowing solvent and other small molecules access to the interior of the protein.

The physiological function of Bet v 1 is basically unknown. Bet v 1 has been classified as a pathogenesis-related protein belonging to the ubiquitous family 10 (PR-10), implicating that Bet v 1 might be involved in the plant defense against microbial attack or in other stress-related situations (*5*, *6*). We have shown that Bet v 1 binds a range of amphiphilic compounds (fatty acids, cytokinins, flavonoids, and sterols) with low μM affinity, suggesting transport or storage activity (*7*). Ligand binding generally involves the cavity (*7*) as confirmed by later studies (*8*, *9*). Other studies imply RNase activity (*10*−*13*). It is not clear if the suggested functions of Bet v 1 are all compatible. The cavity is undoubtedly related to protein function, although it is unclear whether relatively large ligands enter the cavity via instrinsic structural "breathing" or major structural rearrangements of Bet v 1.

A remarkable structural similarity has been found between Bet v 1 and the START domain of MLN64 from man and StarD4 from mouse (*14*, *15*). Both proteins are believed to be cholesterol transfer proteins. The START domains consist of ca. 210 amino acids forming a hydrophobic cavity, which constitutes the putative binding site for cholesterol (*14*). The START domain of the steroidogenic acute regulatory protein (StAR) is predicted to share the same fold (*16*). StAR is

† J.E.M. and D.E.O. are supported by the Villum Kann Rasmussen Foundation (BioNET). D.E.O. and J.J.E. are supported by the Danish Research Foundation (inSPIN).

* Corresponding author. E-mail: dao@bio.aau.dk. Phone: +45 96358525. Fax: +45 98141808.

‡ Aalborg University.

§ Present address: Maxygen ApS, Agern Allé 1, DK-2970 Hørsholm, Denmark.

|| ALK-Abello A/S.

⊥ Aarhus University.

[1] Abbreviations: Bet v 1, the major pollen allergen from birch; DDM, dodecyl maltoside; DOPC, 1,2-dioleyl-*sn*-glycero-3-phosphocholine; DOPE, 1,2-dioleyl-*sn*-glycero-3-phosphoethanolamine; DOPG, 1,2-dioleyl-*sn*-glycero-3-[phospho-*rac*-(1-glycerol)]; LUV, large unilamellar vesicles; lysoMPC, 1-myristoyl-2-hydroxy-*sn*-glycero-3-phosphocholine; lysoMPG, 1-myristoyl-2-hydroxy-*sn*-glycero-3-[phospho-rac-(1-glycerol)]; Mal d 1, the major allergen from apple; MRE, mean residue ellipticity; StAR, steroidogenic acute regulatory protein; START domain, steroidogenic acute regulatory related lipid transfer domain; SUV, small unilamellar vesicles.

10.1021/bi062058h CCC: $37.00
Published on Web 02/21/2007

essential for normal adrenal and gonadal steroidogenesis in mammals, by facilitating the import of cholesterol into mitochondria (*17*). It acts exclusively on the outer membrane to induce the flow of cholesterol to the inner membrane. StAR has been shown to form a molten globule at low pH (*18*). This non-native state is able to associate with phospholipid vesicles in a pH-dependent manner (*19*). The physical−chemical properties of the bilayer were also found to be important for the interaction as the inclusion of cholesterol and negatively charged phospholipids facilitated binding to the membrane (*19*).

Given the structural similarity between the START domain and Bet v 1, the question arises if the allergen also is capable of interacting with membranes. This is highly relevant in view of the unknown natural function of Bet v 1 and its homologues. In this study, we have used synthetic phospholipid vesicles to explore whether Bet v 1 is able to interact with biological membranes. Specifically, we have addressed the following issues: To what extent does the properties of the bilayer affect a possible binding event? What are the consequences on the structure of both the protein and the membrane upon binding? Does Bet v 1 associate superficially with or become inserted into the membrane?

EXPERIMENTAL PROCEDURES

Materials. 1,2-Dioleyl-*sn*-glycero-3-phosphocholine, 1,2-dioleyl-*sn*-glycero-3-phosphoethanol-amine, 1,2-dioleyl-*sn*-glycero-3-[phospho-*rac*-(1-glycerol)], 1-myristoyl-2-hydroxy-*sn*-glycero-3-phosphocholine, and 1-myristoyl-2-hydroxy-*sn*-glycero-3-[phospho-*rac*-(1-glycerol)] were from Avanti Polar Lipids (Alabaster, AL); calcein and pepsin were from Fluka (Busch, Germany); and SDS−PAGE low molecular weight markers were from MBI Fermentas (St. Leon Rot, Germany). All other chemicals were from Sigma Chemical Co. (St. Louis, MO). Nucleopore track etch filters used for lipid extrusion were from Whatman (Maidstone, U.K.). Bet v 1 (isoform 2801) and Mal d 1 (isoform 2620) were purified as described (*20*, *21*). Protein concentrations were determined spectrophotometrically using molar extinction coefficients of 10 430 and 17 880 M^{-1} cm^{-1} at 280 nm for Bet v 1 and Mal d 1, respectively, as calculated from the amino acid sequences (*22*). For pH titration experiments the following buffers were used: pH 2.4−3.8, citrate; pH 4.2−5.1, potassium acetate; pH 6.2−7.2, potassium phosphate; pH 8.1−8.6, TRIS; pH 9.3, borate.

Preparation of Phospholipid Vesicles. Lipids were suspended in Milli Q water by at least 30 s of vortexing, and subjected to 5 rounds of freezing in liquid N_2 and thawing in a water bath at 55 °C before extrusion on a 15 mL thermobarrel extruder (Northern Lipids, Vancouver). Lipid mixtures were dissolved in chloroform and dried on a Speed-Vac at low pressure for at least 6 h before resuspension in Milli Q water and subjection to the freeze/thaw cycle. For formation of LUVs, lipid suspensions were extruded 8 times through 100 nm filters (yielding vesicles with a diameter of 100 nm) followed by extrusion 8 times through 50 nm filters (yielding 50 nm vesicles) at room temperature. SUVs were prepared by sonicating lipid suspensions in an ice-bath with a Sonopuls HD 2070 ultrasonicator (BANDELIN electronic, Berlin, Germany) equipped with a MS73 micro tip mounted on a UW 2070 adaptor for 60 min at 35 W with a 50% pulse cycle. The lipid concentration after extrusion or sonication was typically 11 mM. All vesicles were allowed to equilibrate overnight at 4 °C before use, and were used within 6 days of production.

Far-UV CD Measurements. Far-UV CD wavelength spectra and temperature scans were recorded on a Jasco J-810 spectropolarimeter (Jasco Spectroscopic Co. Ltd., Hachioji City, Japan) equipped with a JASCO PTC-348WI temperature control unit. The ellipticity was measured at 25 °C, and six (lysolipids) or 10 (phospholipids) accumulations were averaged to yield the final spectrum. A 0.1 cm path length cuvette was employed. The protein concentration was 6.9 μM, and the phospholipid and lysophospholipid concentrations were 2 mM and 3 mM, respectively. All measurements were performed in 20 mM buffer as detailed above. Thermal scans were performed with a scan rate of 60 °C/h. The contribution of buffer and lipid to the measured ellipticity was subtracted as blank. All samples were allowed to equilibrate for 30 min prior to measurement. The mean residue ellipticity (MRE) was expressed as deg cm^2 $dmol^{-1}$ $residue^{-1}$ based on molecular masses of 17 405 Da and 159 amino acids and 17 514 Da and 158 amino acids for Bet v 1 and Mal d 1, respectively.

We observed a certain amount of turbidity when Bet v 1 was mixed with DOPC or DOPG vesicles around pH 4. However, we do not believe that this affects our analysis of the CD data, since the wavelength spectra were not significantly different from those of other spectra in the same pH range where the solutions were visually clear. Furthermore, the same types of spectra were obtained with lysophospholipids, where no visible precipitation took place.

Thermal scans were analyzed as described (*28*). The content of secondary structure was deconvoluted from the CD wavelength spectra by four methods, SELCON3, CONTINLL, CDSSTR, and K2D, which are supplied by DICHROWEB at http://www.cryst.bbk.ac.uk/cdweb/html/home.html (*23*). For SELCON3, CONTINLL, and CDSSTR, both reference sets 4 and 7 were used, yielding a total of seven different outputs.

Calcein Release Experiments. Calcein-containing 50 nm vesicles were prepared by resuspending 40 mg of lipid in 1.8 mL of 90 mM calcein in Milli Q water. The suspension was subjected to 5 rounds of freezing in liquid N_2 and thawing in a water bath at 55 °C before extrusion four times through 100 nm filters and 10 times through 50 nm filters. Non-entrapped calcein was removed by running the vesicle samples through a Pharmacia PD-10 gel filtration column and collecting the fraction eluting at 500−1000 μL, which gave the largest change in fluorescence signal upon complete release of calcein by 5% (w/v) Triton X-100. Samples were mixed immediately after collection in a final volume of 400 μL containing 1.7 μM protein, 50 mM buffer, and 8 μL of calcein-containing vesicles. Calcein fluorescence was measured after 15 min of sample equilibration by excitation at 490 nm, following emission at 495−600 nm (slit widths 3 nm) on an LS-55 spectrofluorometer (Perkin-Elmer) in a 1 cm path length cuvette at 25 °C.

Limited Proteolysis. Initially, Bet v 1 or Mal d 1 was mixed with 2 mM (monomer concentration) vesicles or 3 mM micelles in 40 mM buffer, and the samples were equilibrated for 15 min to allow formation of the different conformational states. Subsequently, either trypsin or pepsin was added, and

the samples were incubated for 30 min. The final concentrations of allergen and protease were 11.4 μM and 1.8 μM, respectively, in a total reaction volume of 25 μL. All reactions took place at room temperature. Proteolysis was stopped by the addition of 5 μL of 5x SDS−PAGE sample buffer. Before separation of protein fragments on a 15% tris/tricine gel, samples were boiled for 5 min. Protein was detected by staining with Coomassie Brilliant Blue R-250.

NH_2-Terminal Amino Acid Sequencing. A number of protease-treated Bet v 1 samples were selected for NH_2-terminal amino acid sequencing. Proteolysis was performed as described above. Fragments of Bet v 1 were separated by SDS−PAGE on 5−15% gradient gels using the glycine/2-amino-2-methyl-1,3-propanediol-HCl system (*24*). For this analysis, the stacking gel was allowed to polymerize 1 day prior to electrophoresis and samples were heated for 3 min at 80 °C only. After electrophoresis, proteins were transferred to a polyvinylidene diflouride membrane (Immobilon−P, Millipore) in 10 mM CAPS, 10% (v/v) methanol, pH 11 as described (*25*). Samples were analyzed by automated Edman degradation using a Procise amino acid sequencer (Applied Biosystems) with on-line phenylthiohydantoin analysis by HPLC.

1D-NMR Experiments. All NMR spectra were recorded at 298 K on a BRUKER DRX600 spectrometer operating at a field strength of 14.1 T, equipped with a TXI(H/C/N) probe with triple-axis gradients. Spectra were processed using XWinNMR 3.6. Three samples were measured: 50 μM Bet v 1 in 50 mM potassium phosphate at pH 7.1, 50 μM Bet v 1 in 50 mM potassium phosphate at pH 7.1 containing 25 mM lysoMPC, and 50 μM Bet v 1 in 50 mM potassium phosphate/70 mM citric acid at pH 3.9 containing 25 mM lysoMPC. 1D-NMR spectra of these solutions were measured using excitation-sculpting water suppression (*26*). In the presence of lysoMPC, where signal intensities were much lower (particularly at pH 3.9), the spectra were acquired using selective excitation of the H^N region from 6 to 9 ppm by an off-resonance Q5 pulse (*27*) of 3.14 ms duration in addition to excitation-sculpting water suppression in order to minimize detrimental effects of the strong lysoMPC signals. Still, 8192 (pH7.1) and 16 384 (pH3.85) scans had to be accumulated to obtain spectra. In comparison, 1024 scans (excitation sculpting, but no selective pulse) were sufficient in the absence of detergent.

RESULTS

The objective of this study was to provide a biophysical analysis of the interaction of Bet v 1 with synthetic phospholipid vesicles, which constitute model biological membranes. We focus on both the size and charge of the vesicles in conjunction with pH, in view of the fact that all these parameters are known to play a role for the binding of proteins to vesicles. As spectroscopic technique we use CD rather than fluorescence. Not only is CD more structurally informative, Bet v 1 contains no Trp residues, only 7 Tyr residues, which are rather insensitive to their environment and give very modest fluorescence changes even when Bet v 1 undergoes profound structural changes in connection with unfolding in denaturant (*28*).

Bet v 1 Binds Only to Sonicated DOPC Vesicles and Only at Low pH. In the absence of vesicles, Bet v 1 unfolds at acidic pH with a midpoint around pH 3.6 (*28*). Unfolding proceeds directly to the unfolded state without a stable intermediate, as there is a clear isodichroic point around 208 nm (Figure 1A). The deviations for pH 2.3 below 208 nm may be ascribed to the reduced quality of the data in this region of the spectrum.

This transition is completely unaffected by the presence of 100 and 50 nm zwitterionic (DOPC) vesicles (summarized in Figure 1F); however, when we use sonicated DOPC vesicles, we see a clear difference at pH 4.2 and below compared to the absence of lipids (Figure 1B). Rather than a transition to a random coil-like conformation, a state appears which is rich in α-helical structure, as seen by the characteristic minima at 222 and 208 nm. The α-helix rich state is fully developed at pH 3.3. Thus Bet v 1 is only able to bind to zwitterionic vesicles when the pH is low and the vesicles are small.

Bet v 1 Binds to Both SUV and LUV Vesicles of DOPG. The interaction of Bet v 1 with membranes becomes even more pronounced in the presence of anionic (DOPG) vesicles, where a change is evident already below pH 6.5 when using 100 or 50 nm vesicles (Figure 1C). The structure at pH 5.1 resembles that of Bet v 1 at low pH in SUV DOPC. However, at lower pH, the ellipticity at 208 nm decreases approximately 33%, while leaving the ellipticity at 220 nm unchanged, suggesting that another kind of structure forms. SUV DOPG vesicles reveal structural changes already at pH 7.2 as the CD spectra exhibit an α-helical profile (Figure 1D), although with lower ellipticity compared to SUV DOPC (pH 3.8−2.4) and LUV DOPG (pH 5.1). At intermediate pH (5.1−4.2), the spectra are similar to those in LUV DOPG at the same pH, whereas at lower pH (3.8−2.4), the ellipticity decreases. Thus we conclude that there are at least two different states of Bet v 1 bound to vesicles, and that conformational changes are encouraged by an increase in vesicle curvature (presumably due to the formation of small defects in the vesicle surface, cf. refs *29*, *30*) and an increase in anionic surface charge, which encourages electrostatic attractions at low pH where Bet v 1 (pI ∼ 5.4) is positively charged.

The Binding of Bet v 1 to Vesicles Is a Reversible Process. When Bet v 1 is initially brought to low pH in the presence of DOPG or DOPC and then returned to neutral pH (still in the presence of lipids), the CD spectrum at neutral pH is identical to that of Bet v 1 which has not been exposed to low pH (data not shown). This shows that binding of Bet v 1 to vesicles and the concomitant structural changes are completely reversible and do not kinetically trap Bet v 1 in certain states.

The Micelle-Forming Lysophospholipids, LysoMPC and LysoMPG, Also Promote Structural Changes in Bet v 1. Binding of Bet v 1 to phospholipid vesicles is insensitive to the lateral pressure in the lipid head group region of the bilayer, since the CD wavelength spectra are unaffected by the presence of DOPE, a non-bilayer lipid known to encourage negative curvature in the vesicles (*31*) (data not shown). This could indicate that a canonical bilayer environment is not a prerequisite for binding and folding. Therefore we examined the structure of Bet v 1 in the presence of the micelle-forming lysophospholipids lysoMPC and lysoMPG. Binding to these detergent lipids is clearly enhanced compared to the vesicle-forming lipids; clear induction of

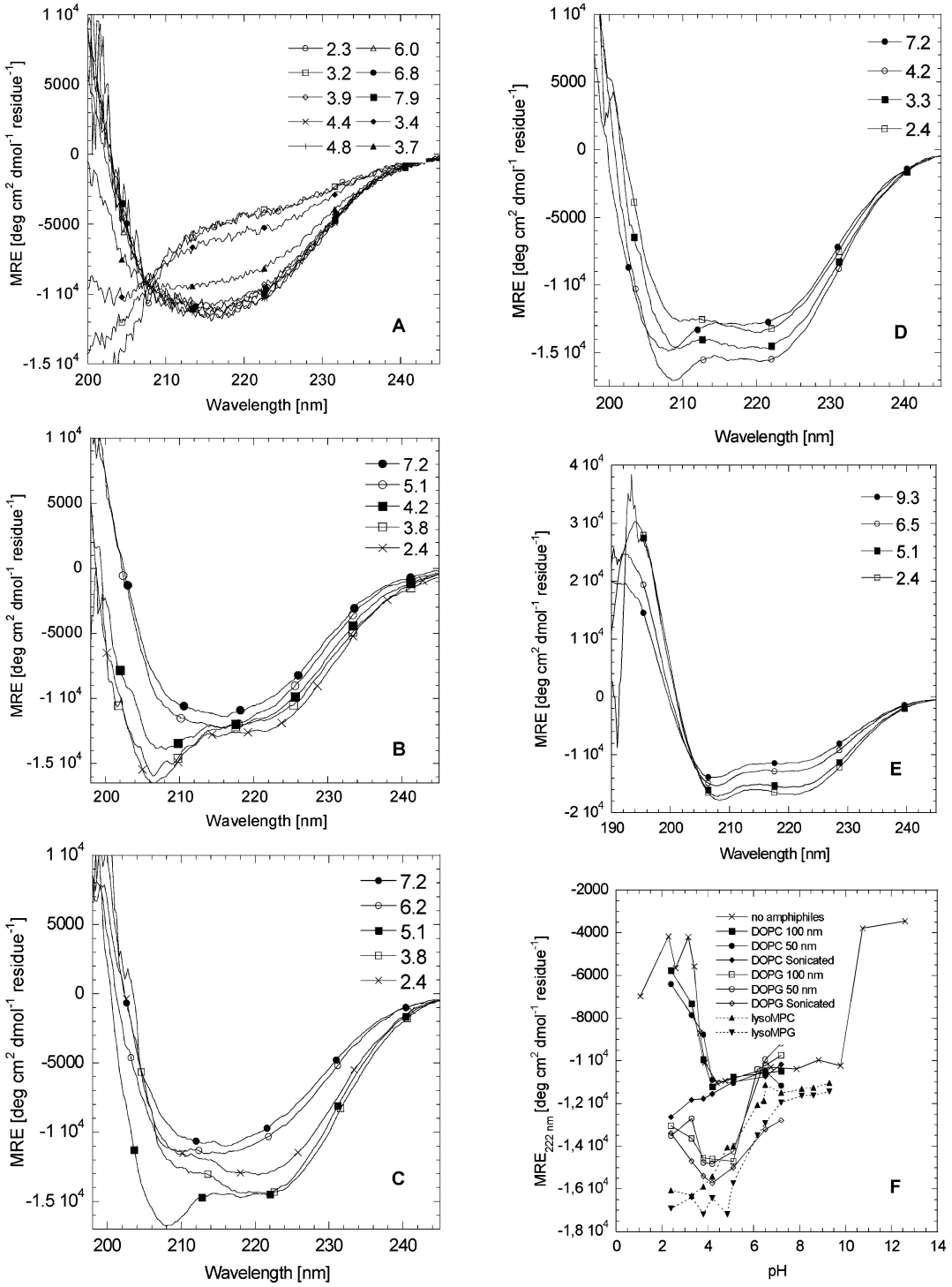

FIGURE 1: Far-UV CD spectra of Bet v 1 in (A) the absence of lipids at different pH values, (B) sonicated DOPC vesicles, (C) 100 and 50 nm DOPG vesicles, (D) SUV DOPG vesicles, and (E) lysoMPC and lysoMPG micelles. (F) Summary of CD molar ellipticity at 222 nm as a function of pH. The CD spectra could be recorded down to 190 nm for lysolipid micelles due to reduced light scattering.

α-helical structure is observed at all pH values (up to 9.3), and there is an increase in ellipticity with lowered pH with a cooperative transition centered around pH 5 (Figure 1E**)**. NMR spectra of Bet v 1 in the presence of lysoMPC also support the occurrence of structural changes and interaction with lipids, as discussed below under "The A- and B-States Are Partially Unfolded".

Although both detergents induce α-helical structure in Bet v 1, titration with varying mole proportions of lysoMPG and lysoMPC reveals a ca. 30% increase in ellipticity at pH 5.1 as the lysoMPG mole fraction increases from 0 to 100%. However, this only reflects a shift in the midpoint of the pH titration curve in the two detergents. The ellipticity values at the end points (pH ∼8 and pH ∼3) (Figure 1F) are virtually identical for the two different detergents.

All the observed effects only occur above the cmc of the detergents (0.06 and 0.3 mM for lysoMPC and lysoMPG, respectively, in 50 mM TRIS, pH 8, 25 °C (*32*)), indicating that Bet v 1 needs to bind to an interface rather than to amphipathic monomers (data not shown). Titration of Bet v 1 with lysoMPC shows that the ellipticity values (shown for 222 nm in Figure 2) decrease steeply between 0 and 0.5 mM.

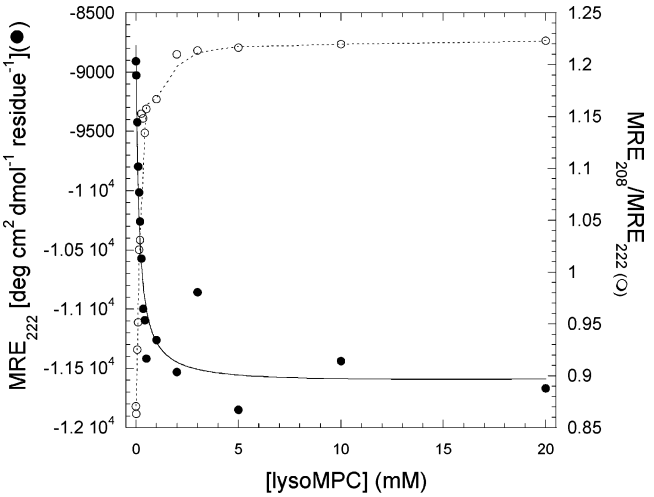

FIGURE 2: Titration of Bet v 1 with lysoMPC monitored by ellipticity at 222 nm and the ratio between ellipticities at 208 and 222 nm. The joined line is the best fit to a binding isotherm. This gives an apparent binding constant K_d of 0.15 ± 0.05 mM. The stippled line for the ratio data is included to guide the eye.

Fitting the ellipticity data at 222 nm to a binding isotherm yields an apparent binding constant of 0.15 ± 0.05 μM. An identical K_d value was obtained using ellipticity data at 208 nm. The ratio of the ellipticities at the two minima (208 and 222 nm) also reveals a plateau around 0.5 mM (Figure 2). Thus the signal increases smoothly from 0 mM lysoMPC without any clear breakpoint around the cmc. The interaction with lysoMPC is not driven by electrostatic interactions, since the addition of up to 4 M NaCl, which would screen such interactions, had no effect on the structural changes of Bet v 1 (data not shown).

The Nonionic Detergent Dodecyl Maltoside Does Not Support Structural Changes in Bet v 1. The head group structure of the lipids/detergents must play a very significant role in promoting Bet v 1 membrane binding, since no structural changes are seen in the presence of the nonionic detergent dodecyl maltoside at pH 7.2 (Figure 3A). Importantly, addition of the anionic detergent SDS led to an α-helical structure, which, however, is distinct from that in lysoMPC, with shifts in the positions of the two minima and reduced ellipticity (Figure 3A). Thus, the structural changes observed for Bet v 1 in the presence of lysoMPC and lysoMPG are not just the results of detergent-mediated unfolding as seen with SDS in other contexts (*33*, *34*).

Global Analysis of CD Wavelength Spectra for Identification of Common States. At this stage we find it useful to introduce a classification of the "archetypal" states, which Bet v 1 can form in the presence of the different membrane-like environments investigated. Based on a comparison of the different CD spectra, we identify four different states (Figure 3B), which we here term N (native), A, and B, in addition to the denatured state D. These archetypal CD spectra were deconvoluted using SELCON3, CONTINLL, CDSSTR, and K2D to obtain the secondary structure distribution of Bet v 1 (see Experimental Procedures for details). Table 1 shows the conditions under which these states are formed and their estimated content of secondary structure. The absolute values of these predictions should be approached with caution, due to the significant deviation between the secondary structure values in the crystal structure and the predicted value for the native state. Therefore we will use the figures in Table 1 as an indication of the trends in structural changes, rather than as absolute estimates of

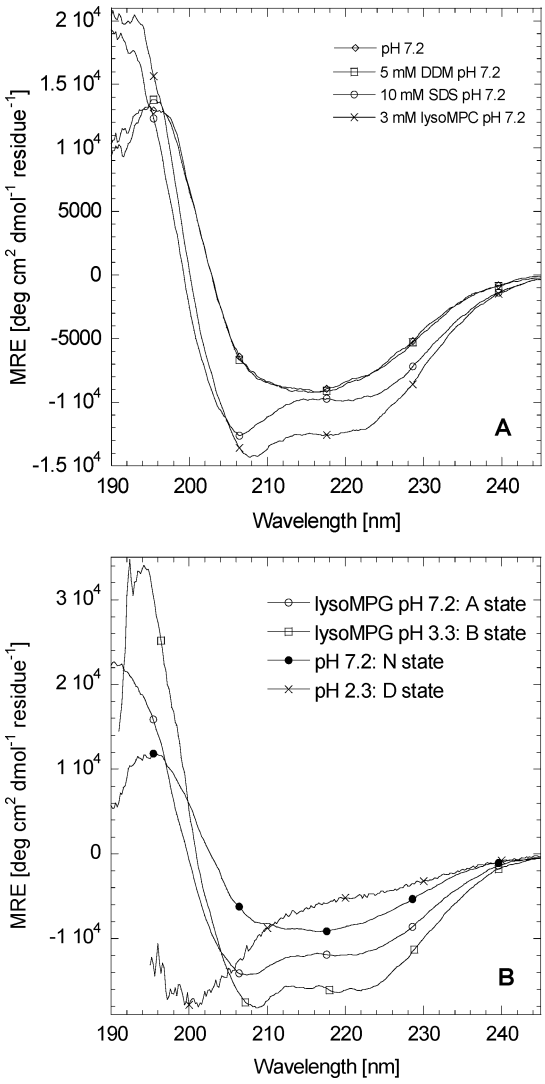

FIGURE 3: Representative CD spectra of different states of Bet v 1 in (A) different detergents and (B) different lipids.

Table 1: Results of Secondary Structure Estimation as Predicted from Far-UV CD Wavelength Spectra

state	secondary structure content[a]	conditions
N[b]	28% α 26% β 47% unordered	pH 4−10
A	37% α 15% β 48% unordered	lysoMPC pH 9.5−7; lysoMPG pH 9.5−7; sonicated DOPG pH 7.2−6.5; sonicated DOPC pH 2.4
B	57% α 7% β 35% unordered	lysoMPC pH 4.2−2.4; lysoMPG pH 4.2−2.4; sonicated DOPG pH 5.1−4.2; 100 nm DOPG pH 5.1; 50 nm DOPG pH 5.1

[a] Average of estimates from K2D, SELCON3 (reference sets 4 and 7), CONTINLL (reference sets 4 and 7), and CDSSTR (reference sets 4 and 7). All programs use spectra over the range 190−245 nm except K2D (200−245 nm). The relative standard deviation on the structural element prediction is typically 5−15%. The lowest relative standard deviations are not associated with a particular structural element. [b] The crystal structure of Bet v 1 shows that the native protein contains approximately 28% α-helix, 40% β-structure, and 32% other (*4*).

the structural content. Nevertheless, it is clear that A and B are different from the N state due to the significant increase in ellipticity and the appearance of two distinct minima around 207(A)/209(B) nm and 222 nm, which is reflected in the progressive increase in α-helicity and decline of *β*-sheet structure (Table 1). The minimum at 208 nm is for both A and B lower than that at 222 nm. It has been noted for water-soluble α-helical proteins that a 222/208 ratio greater than 1 is typical of coiled-coil (*35*, *36*) structures, whereas a ratio smaller than 1 indicates monomeric or separate helices (*37*). Analogous observations can be made for α-helical membrane proteins in the native state versus the SDS-denatured state (*38*). This suggests that the A and B states contain an increased amount of fluctuating α-helical structure. In addition to these four states, the state formed in sonicated DOPG vesicles at pH 2.4 has a distinct spectrum which cannot be reconstructed satisfactorily by combining spectra from the B- and the N-states (data not shown). However, since it is only formed under a very narrow range of conditions, it will not be investigated further here.

It is evident from the deconvolution analysis that in the bound states α-helical structure develops at the expense of *β*-sheet structure. In the A-state, the α-helical content is increased from 26% (in the natively folded state) to 37%, whereas it amounts to 57% in the B-state (see Table 1). Concomitantly, the *β*-sheet content decreases from 27% (based on prediction) to 15% in the A-state and only amounts to 7% in the B-state (see Table 1).

Having identified a number of different conformational states of Bet v 1 in the presence of different lipids, we next sought to characterize these states in terms of (a) their degree of structural mobility and (b) their effect on membrane structure.

The A- and B-States Are Partially Unfolded. It is evident from the analysis of the CD wavelength spectra of Bet v 1 that the protein undergoes dramatic changes in structure upon interaction with the vesicles or micelles. Therefore we wanted to investigate if the bound states are cooperative entities, containing dominant tertiary interactions, or if they are partially unfolded, having lost most tertiary contacts and are stabilized primarily by secondary structure. NMR spectra of partially unfolded proteins are much less dispersed than those of a native protein and resemble the spectrum of a denatured protein (*39*). Due to increased molecular mobility, unfolded states usually show narrower lines in the NMR spectra than folded states. 1D-NMR spectra of Bet v 1 in the absence and presence of lysoMPC revealed significant structural changes between the native state (pH 7.2) and the two states found on either side of the transition around pH 5 (B-state at pH 3.85 and A-state at pH 7.2 both in lysoMPC) (Figure 4A). Under both conditions there is a clear loss of tertiary structure, as seen by the decrease in signal dispersion, indicating that both the B-state and the A-state are non-native states. However, this loss of tertiary structure is not coupled to a narrowed line width; in fact, rather the opposite is the case, the line widths of the NMR signals seem to increase. Concomitantly, the signal-to-noise ratio drops. This points toward reduced molecular mobility as occurs when the protein is bound to a large particle, e.g., a micelle.

The loss of tertiary structure in the B- and A-states seen by NMR is corroborated by thermal scans monitored by CD (Figure 4B). A native structure will give rise to a sharp

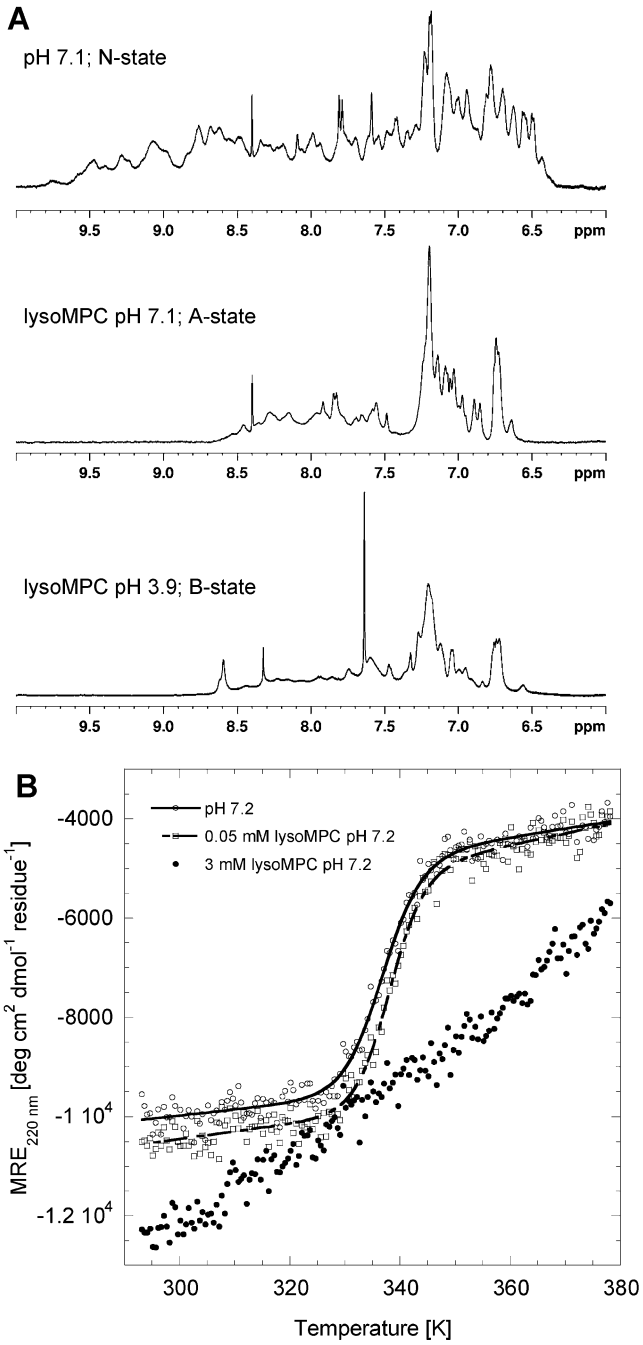

FIGURE 4: (A) NMR spectra of Bet v 1 in the absence (1024 transients accumulated) and presence of lysoMPC (8192 transients at pH7.1 and 16 384 transients at pH3.9 accumulated). (B) Thermal scans monitoring the ellipticity of Bet v 1 at 220 nm at different concentrations of lysoMPC. The joined curves at 0 and 0.05 mM lysoMPC represents the best fits of the data to a two-state unfolding transition (*28*).

transition within a relatively narrow temperature range (10−15 °C), whereas a fluctuating conformation will show a more gradual loss of structure with increasing temperature. We tested the thermal stability of Bet v 1 at pH 7.2 in lysoMPC concentrations below (native state) and above (A-state) its cmc. In the presence of monomeric lysoMPC, Bet v 1 unfolds with a sharp transition around 68 °C characteristic of native Bet v 1 (Figure 4B) (*28*). However, in the presence of micellar lysoMPC, a gradual decrease in signal is observed, which is not complete at 105 °C. These data suggest that the A-state has lost its cooperative nature, thus corroborating

Table 2: Permeabilization of DOPG Vesicles by Bet v 1 under Different Conditions Measured by Calcein Release

vesicle size	pH	state of Bet v 1	permeabilization
50 nm	7.2	N	0
sonicated	7.2	A	7%
50 nm	5.1	B	96%

the data obtained by NMR. A non-cooperative loss of structure is indicative of partially folded proteins with isolated elements of secondary structure.

The B-State but Not the A-State Is Able To Permeabilize Membranes. The effect of Bet v 1 binding on membrane structure and integrity can be analyzed by calcein release experiments. The fluorescent probe calcein self-quenches at high concentrations, e.g., when trapped inside vesicles. Dilution of the probe by leakage from the vesicle lumen will increase fluorescence. Complete leakage is obtained by the addition of high concentrations of detergent. There is no change in calcein fluorescence in 50 nm DOPG vesicles at pH 7.2 in the presence of Bet v 1 (Table 2). This is in agreement with the finding that no structural transitions of the native state occur under these conditions. However, complete leakage of the probe is observed by the B-state formed at pH 5.1. In contrast, the A-state (formed with sonicated DOPG vesicles at pH 7.2) cannot induce any significant leakage. Apparently, although both the B- and the A-states are non-native, only the B-state perturbs the structure of the bilayer. Nevertheless, under all conditions the vesicles retain their overall structural integrity and do not fragment into smaller pieces according to dynamic light scattering experiments (data not shown).

Limited Proteolysis Indicates Different Conformational Flexibility. In order to test the conformational flexibility of the different conformational states of Bet v 1 in the presence and absence of lipids, we incubated the protein with trypsin (pH range 7.2−5.1) or pepsin (pH range 4.2−3.3) and separated the degradation products on Tris/Tricine gels. The proteases show different specificities, trypsin cleaving after Arg or Lys residues (18 sites on Bet v 1) and pepsin mainly after Phe, Leu, and Glu (31 sites on Bet v 1). However, in both cases there are so many potential cleavage sites that we can assume that any flexible region of the protein will be cleaved by the protease, allowing us to compare the overall effects of the two different proteases. As positive controls of degradation, we used the conformationally flexible proteins BSA and α-lactalbumin. These two proteins were degraded under all conditions tested in terms of pH and lipid species, although the glycerol-containing lipids had a slight inhibitory effect on pepsin activity (data not shown). In the absence of lysoMPC at pH 7.2, native Bet v 1 is completely resistant to trypsin degradation, whereas at pH 4.2, the protein is completely degraded by pepsin (Figure 5). Although Bet v 1 retains its native structure at pH 4.2, the overall conformation of the protein is more dynamic and flexible or a sufficient fraction is unfolded to allow rapid degradation. In the presence of lysoMPC at pH 7.2 (A-state), the protein is degraded by trypsin resulting in a diffuse degradation pattern; however, at pH 4.2 (B-state) a well-defined fragment of ca. 13 kDa accumulates. Performing the proteolysis experiments using both sonicated and extruded DOPC and DOPG vesicles yielded similar results, although the protected fragments from the B-state varied slightly in size (10−15 kDa) depending on the exact conditions used (see Table 3). The limited proteolysis assay reveals that the B-state is better protected against protease attack than the A-state. One explanation for this could be that the B-state is inserted deeper into the bilayer thus preventing a general

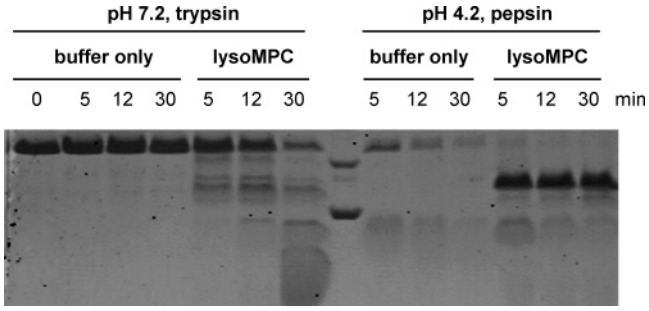

FIGURE 5: Proteolysis of Bet v 1 at pH 7.2 and 4.2 by trypsin and pepsin, respectively.

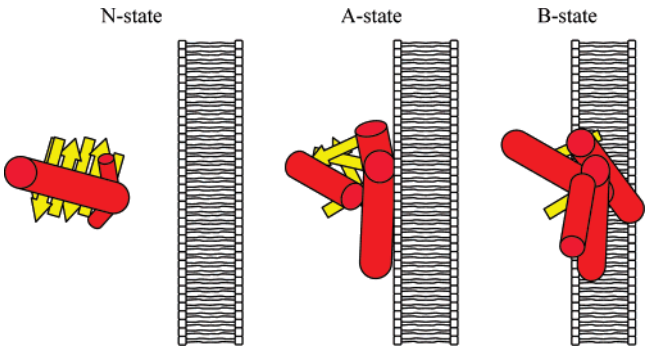

FIGURE 6: Schematic of the Bet v 1 N-, A-, and B-states. The red and yellow structures represent Bet v 1; the black structures represent a phospholipid bilayer.

Table 3. Overview of Data from Limited Proteolysis and NH_2-Terminal Sequencing

Bet v 1 state	pH[a]	lipid	proteolysis	NH_2-terminal sequence
N	7.2	none	fully protected	nd
	4.2	none	fully degraded	nd
	7.2	100 nm DOPG	fully protected	nd
	7.2	100 nm DOPC	fully protected	nd
	7.2	sonicated DOPC	fully protected	nd
	6.5	100 nm DOPC	fully protected	nd
	5.1	100 nm DOPC	fully protected	nd
A	7.2	lysoMPC	fully degraded	nd
	7.2	lysoMPG	fully degraded/ diffuse fragments	
			∼14 kDa	V_{33}APQAI
			∼11 kDa	V_{33}APQAI
			∼7 kDa	V_{33}APQAI + K_{55}ISPFE
			∼4 kDa	K_{55}ISPFE
	7.2	sonicated DOPG	fully degraded	nd
B	5.1	100 nm DOPG	protected fragment	
			∼15 kDa	G_1VFNYE + V_{33}APQAI
	5.1	sonicated DOPG	protected fragment	
			∼15 kDa	G_1VFNYE
	4.2	sonicated DOPG	fully protected	nd
	3.8	lysoMPG	fully protected	nd
	3.8	lysoMPC	protected fragment	
			∼14 kDa	G_1VFNYE + N_4YETET
C	3.8	sonicated DOPC	fully degraded	nd

[a] Trypsin is used in the pH range 7.2−5.1; pepsin is used in the pH range 4.2−3.8.

degradation of the polypeptide chain. This is in agreement with the calcein release data (Table 2) where only the B-state releases calcein, due to a severe perturbation of the membrane. The NMR data, showing an increased line width and decreased signal-to-noise ratio of the B-state as compared to the A-state (Figure 4A), also support this explanation.

To investigate which part of Bet v 1 contacts the membrane in the B-state, we subjected the protected fragments to NH_2-terminal amino acid sequencing. This analysis revealed the following sequences: G_1VFNYE and N_4YETET in lysoMPC pH 3.8; G_1VFNYE in sonicated DOPG vesicles pH 5.1; and G_1VFNYE and V_{33}APQAI in 100 nm DOPG vesicles. Thus it appears that the C-terminal part of B-state Bet v 1 is exposed, while the N-terminal part of the protein is generally shielded by the interaction with the membrane, though to a lesser extent in large DOPG vesicles.

Although proteolysis of the A-state generally led to diffuse fragments (Figure 5), in lysoMPG at pH 7.2 four identifiable fragments appeared. These fragments were amenable for sequencing yielding V_{33}APQAI and K_{55}ISFPE (Table 3), indicating that the N-terminus is exposed. However, the size of the fragments was smaller than expected for the 33−159 and 55−159 fragments implying C-terminal cleavage as well. The susceptible Lys32−Val33 and Lys54−Lys55 bonds are located in the C-terminal part of the minor α-helix and the middle of *β*-strand 3, respectively. These structures do not constitute readily accessible cleavage sites in the native state, as indicated by the resistance to trypsin degradation in the absence of membranes. This observation shows that the protein undergoes a conformational change upon binding to the membrane. However, the absence of calcein leakage from the vesicles (Table 2) indicates that the protein associates with the membrane without disrupting its integrity.

The Homologous Protein Mal d 1 Is Also a Membrane Binding Protein. The Bet v 1 homologue Mal d 1 (the major allergen from apple), which shares 59% sequence homology to Bet v 1, has the same ability as Bet v 1 to undergo structural changes in the presence of lysoMPG and lysoMPC (data not shown). In addition, it also permeabilizes DOPG vesicles in the B-state (but to a slightly lesser extent than Bet v 1) and not the A-state (data not shown). This indicates that it is the overall fold shared by these two proteins, namely an α/*β* fold with a large water-filled tunnel, that facilitates binding and structural rearrangements.

DISCUSSION

Interaction of Bet v 1 with Membranes. The far-UV CD experiments identify several factors that mediate binding of Bet v 1 to membranes: electrostatic attraction, vesicle curvature (and hence surface cracks/defects), and partial unfolding (at low pH). Bet v 1 only binds to DOPC vesicles with high vesicle curvature and only at very low pH. Since DOPC is zwitterionic, simple electrostatic attraction is not adequate to induce binding, so under these conditions Bet v 1 has to be unfolded since binding only starts at a pH where it will normally unfold. Even then binding only occurs when it can attack via cracks/defects on the vesicle surface due to sharp curvature (*40*−*42*). When the vesicles are negatively charged (DOPG), electrostatics facilitate binding, which commences at pH 5.1 (extruded vesicles) and already at pH 7 when combined with sharp curvature defects (sonicated vesicles), and it becomes even more pronounced at low pH. In the case of lysoMPC, micelle dynamics and flexibility make up for lack of charge, but also here low pH unfolding increases the conformational change.

Consequences of Binding on Protein and Membrane Structure. Binding of Bet v 1 to membranes is accompanied by an increase in α-helical content at the expense of *β*-strand structure, presumably due to the formation of amphipathic helices in the lipid interfacial region. Although the bound forms are highly structured, they are partially denatured in the sense that they have lost their cooperative nature and hence have few tertiary interactions. Although we cannot exclude the existence of other states formed, e.g., in sonicated DOPG vesicles at low pH, we consider the A- and the B-states the most important as they can be formed both in micelles and DOPG vesicles and occur at neutral to intermediate pH (from 9 down to 4).

We cannot exclude that the A-state is an intermediate on the pathway to the B-state that does not fully develop because the optimal "interaction conditions" are not provided (see previous section). The A-state is less α-helical than the B-state, is more sensitive to degradation, which predominantly happens from the N-terminus, and is not able to induce calcein release from the vesicles. Thus, the B-state represents the fully developed state in the sense that it displays the largest change in structure and that it at least partially penetrates the vesicle structure, which may be physiologically relevant (see below).

Besides changes in protein structure, the binding event also affects membrane structure. This was only found for the B-state, which is able to cause full release of calcein from the vesicles. Although the integrity of the bilayer is impeded by the binding of the protein, the overall architecture of the vesicles is intact as revealed by dynamic light scattering experiments. We do not know if Bet v 1 is bound in a monomeric state or if it forms oligomers on the vesicle surface. However, the retention of overall membrane integrity means that we can narrow down its mode of activity. Antimicrobial peptides can permeabilize membranes by forming barrel-stave pores, which retain membrane integrity, or by the carpet model which effectively solubilizes the membrane (*43*). Thus the carpet model can be excluded as a possible mode of activity for Bet v 1.

Functional Implications of Membrane Binding. One of the most pertinent issues in studying the properties of Bet v 1 is to understand its biological function. So far different functions have been proposed, the two most important being RNase activity (*10*, *11*) and general ligand binding (*7*). Here, we add a new dimension to the possible functions that Bet v 1 could have by showing that it is a membrane binding protein. The question then arises if membrane binding is coupled to ligand binding? For instance, could Bet v 1 pick up ligands by binding to the membrane followed by structural rearrangements, which allow entry of ligand to the cavity? Bet v 1 binds ligands that may be too bulky to enter the cavity directly via its openings to the protein surface, and therefore some degree of structural alterations could be required for ligand entry. Indeed, for StAR it has been shown that the large C-terminal helix, which creates the floor in the cavity, is central for membrane and ligand binding (*44*). By engineering disulfide bonds into the protein that restricts the mobility of the C-terminal helix, it was shown that the

ability to bind to both membranes and ligands was eliminated, implying that a structural transition is required for these activities. Although there are many similarities between the properties of StAR and Bet v 1, there are also important differences. StAR is able to form a molten globule at low pH in the absence of a membrane (*18*), which is not the case for Bet v 1. Furthermore, although the N-terminal region 63−193 is able to bind to phospholipid membranes (*45*), it is the C-terminal part (the large C-terminal α-helix) of StAR that is most intimately in contact with the membrane according to proteolysis studies (*46*), whereas for Bet v 1 it seems to be the N-terminus.

One question that remains to be addressed is whether ligand binding can influence membrane interaction, i.e., will ligand-bound Bet v 1 act in the same way toward membranes? If the interaction with the membrane has any biological significance, it may be controlled/triggered by ligand binding/dissociation. As far as we can tell from our data, Bet v 1 alone binds reversibly to membranes without penetration to the other side, but ligand binding could conceivably facilitate translocation. Whether Bet v 1 acts as a monomer or oligomer on the membrane, its ability to release calcein could be modulated by ligands, either by blocking a putative pore formed by the monomer or by inhibiting oligomerization in the membrane. Such mechanisms could be exploited in signaling pathways during tissue development from pollen to mature plant. Coincidentally, it might also provide a mechanism to allow Bet v 1 to cross the mucosal lining and become internalized, facilitating an allergic reaction. Although speculative, these are important issues that future studies must address.

REFERENCES

1. Jarolim, E., Rumpold, H., Endler, A. T., Ebner, H., Breitenbach, M., Scheiner, O., and Kraft, D. (1989) IgE and IgG antibodies of patients with allergy to birch pollen as tools to define the allergen profile of Betula verrucosa, *Allergy 44*, 385−395.
2. Ipsen, H., and Løwenstein, H. (1983) Isolation and immunochemical characterization of the major allergen of birch pollen (Betula verrucosa), *J. Allergy Clin. Immunol. 72*, 150−159.
3. Larsen, J. N. (1995) Isoallergens−Significance in Allergen Exposure and Response, *ACI News 7*, 141−146, 160.
4. Gajhede, M., Osmark, P., Poulsen, F. M., Ipsen, H., Larsen, J. N., van Neerven, R. J. J., Schou, C., Løwenstein, H., and Spangfort, M. D. (1996) X-ray and NMR structure of Bet v 1, the origin of birch pollen allergy, *Nat. Struct. Biol. 3*, 1040−1045.
5. Breiteneder, H., Pettenburger, K., Bito, A., Valenta, R., Kraft, D., Rumpold, H., Scheiner, O., and Breitenbach, M. (1989) The gene encoding for the major birch pollen allergen BetvI, is highly homologous to a pea disease resistance response gene, *EMBO J. 8*, 1935−1938.
6. van Loon, L. C., and van Strien, E. A. (1999) The families of pathogenesis-related proteins, their activities, and comparative analysis of PR-1 type proteins, *Physiol. Mol. Plant Pathol. 55*, 85−97.
7. Mogensen, J. E., Wimmer, R., Larsen, J. N., Spangfort, M. D., and Otzen, D. E. (2002) The Major Birch Allergen, Bet v 1, Shows Affinity for a Broad Range of Physiological Ligands, *J. Biol. Chem. 277*, 23684−23692.
8. Markovic-Housley, Z., Degano, M., Lamba, D., von Roepenack-Lahaye, E., Clemens, S., Susani, M., Ferreira, F., Scheiner, O., and Breiteneder, H. (2003) Crystal Structure of a Hypoallergenic Isoform of the Major Birch Pollen Allergen Bet v 1 and its Likely Biological Function as a Plant Steroid Carrier, *J. Mol. Biol. 325*, 123−33.
9. Koistinen, K. M., Soininen, P., Venalainen, T. A., Hayrinen, J., Laatikainen, R., Perakyla, M., Tervahauta, A. I., and Karenlampi, S. O. (2005) Birch PR-10c interacts with several biologically important ligands, *Phytochemistry 66*, 2524−33.
10. Bufe, A., Spangfort, M. D., Kahlert, H., Schlaak, M., and Becker, W.-M. (1996) The major birch pollen allergen, Bet v 1, shows ribonuclease activity, *Planta 199*, 413−415.
11. Swoboda, I., Hoffmann-Sommergruber, K., O'Riordain, G., Scheiner, O., Heberle-Bors, E., and Vicente, O. (1996) Bet v 1 proteins, the major birch pollen allergens and members of a family of conserved pathogenesis-related proteins, show ribonuclease activity in vitro, *Physiologia Plantarium 96*, 433−438.
12. Moiseyev, G. P., Fedoreyeva, L. I., Zhuravlev, Y. N., Yasnetskaya, E., Jekel, P. A., and Beintema, J. J. (1997) Primary structures of two ribonucleases from ginseng calluses. New members of the PR-10 family of intracellular pathogenesis-related plant proteins, *FEBS Lett. 407*, 207−210.
13. Bantignies, B., Séguin, J., Muzac, I., Dédaldéchamp, F., Gulick, P., and Ibrahim, R. (2000) Direct evidence for ribonucleolytic activity of a PR-10-like protein from white lupin-roots, *Plant Mol. Biol. 42*, 871−881.
14. Tsujishita, Y., and Hurley, J. H. (2000) Structure and lipid transport mechanism of a StAR-related domain, *Nat. Struct. Biol. 7*, 408−414.
15. Romanowski, M. J., Soccio, R. E., Breslow, J. L., and Burley, S. K. (2002) Crystal structure of the Mus musculus cholesterol-regulated START protein 4 (StarD4) containing a StAR-related lipid transfer domain, *Proc. Natl. Acad. Sci. U.S.A. 99*, 6949−6954.
16. Mathieu, A. P., Fleury, A., Ducharme, L., Lavigne, P., and LeHoux, J. G. (2002) Insights into steroidogenic acute regulatory protein (StAR)-dependent cholesterol transfer in mitochindria: evidence for molecular modelling and structure-based thermodynamics supporting the existence of partially unfolded states of StAR, *J. Mol. Endocrinol.*, 29.
17. Stocco, D. M., and Clark, B. J. (1996) Role of the steroidogenic acute regulatory protein (StAR) in steroidogenesis, *Biochem. Pharmacol. 51*, 197−205.
18. Bose, H. S., Whittal, R. M., Baldwin, M. A., and Miller, W. L. (1999) The active form of the steroidogenic acute regulatory protein, StAR, appears to be a molten globule, *Proc. Natl. Acad. Sci. U.S.A. 96*, 7250−7255.
19. Christensen, K., Bose, H. S., Harris, F. M., Miller, W. L., and Bell, J. D. (2001) Binding of Steroidogenic Acute Regulatory Protein to Synthetic Membranes Suggests an Active Molten Globule, *J. Biol. Chem. 276*, 17044−17051.
20. Spangfort, M. D., Ipsen, H., Sparholt, S. H., Aasmul-Olsen, S., Larsen, M. R., Mørtz, E., Roepstorff, P., and Larsen, J. N. (1996) Characterization of Purified Recombinant Bet v 1 with Authentic N-Terminus, Cloned in Fusion with Maltose-Binding Protein, *Protein Expression Purif. 8*, 365−373.
21. Holm, J., Baerentzen, G., Gajhede, M., Ipsen, H., Larsen, J. N., Lowenstein, H., Wissenbach, M., and Spangfort, M. D. (2001) Molecular basis of allergic cross-reactivity between group 1 major allergens from birch and apple, *J. Chromatogr. B. Biomed. Sci. Appl. 756*, 307−313.
22. Pace, C. N., Vajdos, F., Fee, L., Grimsley, G., and Gray, T. (1995) How to measure and predict the molar absorption coefficient of a protein, *Protein Sci. 4*, 2411−23.
23. Whitmore, L., and Wallace, B. A. (2004) DICHROWEB, an online server for protein secondary structure analyses from circular dichroism spectroscopic data, *Nucleic Acids Res. 32*, W668−73.
24. Bury, A. F. (1981) Analysis of protein and peptide mixtures. Evaluation of three sodium dodecyl sulfate-polyacrylamide gel electrophoresis buffer systems, *J. Chromatogr. 213*, 491−500.
25. Matsudaira, P. (1987) Sequence from picomole quantities of proteins electroblotted onto polyvinylidene difluoride membranes, *J. Biol. Chem. 262*, 10035−8.
26. Hwang, T. L., and Shaka, A. J. (1995) Water Suppression that Works. Excitation Sculpting Using Arbitrary Wave-Forms and Pulsed-Field Gradients, *J. Magn. Reson. A 112*, 275−279.
27. Emsley, L., and Bodenhausen, G. (1992) Optimisation of shaped selective pulses for NMR using a quaternion description of their overall propagators, *J. Magn. Reson. 97*, 135−148.
28. Mogensen, J. E., Ipsen, H., Holm, J., and Otzen, D. E. (2004) Elimination of a misfolded folding intermediate by a single point mutation, *Biochemistry 43*, 3357−67.
29. Basanez, G., Nieva, J. L., Goni, F. M., and Alonso, A. (1996) Origin of the lag period in the phospholipase C cleavage of phospholipids in membranes. Concomitant vesicle aggregation and enzyme activation, *Biochemistry 35*, 15183−7.

30. Wilschut, J. C., Regts, J., Westenberg, H., and Scherphof, G. (1978) Action of phospholipases A2 on phosphatidylcholine bilayers. Effects of the phase transition, bilayer curvature and structural defects, *Biochim. Biophys. Acta 508*, 185−96.
31. Curran, A. R., Templer, R. H., and Booth, P. J. (1999) Modulation of Folding and Assembly of the Membrane Protein Bacteriorhodopsin by Intermolecular Forces within the Lipid Bilayer, *Biochemistry 38*, 9328−9336.
32. Mogensen, J. E., Sehgal, P., and Otzen, D. E. (2005) Activation, inhibition, and destabilization of Thermomyces lanuginosus lipase by detergents, *Biochemistry 44*, 1719−30.
33. Otzen, D. E., and Oliveberg, M. (2002) Burst-phase Expansion of Native Protein Prior to Global Unfolding in SDS, *J. Mol. Biol. 315*, 1231−1240.
34. Otzen, D. E. (2002) Protein Unfolding in Detergents: Effect of Micelle Structure, Ionic Strength, pH, and Temperature, *Biophys. J. 83*, 2219−30.
35. Zhou, N. E., Kay, C. M., and Hodges, R. S. (1992) Synthetic model proteins. Positional effects of interchain hydrophobic interactions on stability of two-stranded a-helical coiled-coils, *J. Biol. Chem. 267*, 2664−2670.
36. Lau, S. Y., Taneja, A. K., and Hodges, R. S. (1984) Synthesis of a model protein of defined secondary and quaternary structure. Effect of chain length on the stabilization and formation of two-stranded a-helical coiled-coils, *J. Biol. Chem. 259*, 13253−13261.
37. Lazarova, T., Brewin, K. A., Stoeber, K., and Robinson, C. R. (2004) Characterization of peptides corresponding to the seven transmembrane domains of human adenosine A2a receptor, *Biochemistry 43*, 12945−12954.
38. Otzen, D. E. (2003) Folding of DsbB in mixed micelles: A kinetic analysis of the stability of a bacterial membrane protein, *J. Mol. Biol. 330*, 641−649.
39. Ptitsyn, O. B. (1995) Molten globule and protein folding, *Adv. Protein Chem. 47*, 83−229.
40. Wilschut, J. C., Regts, J., Westernberg, H., and Scherphof, G. (1978) Action of phospholipases A2 on phosphatidylcholine bilayers. Effects of the phase transition, bilayer curvature and structural defects. *Biochim. Biophys. Acta 508*, 185−196.
41. Lawaczeck, R., Kainosho, M., and Chan, S. I. (1976) The formation and annealing of structural defects in lipid bilayer vesicles, *Biochim. Biophys. Acta 443*, 313−330.
42. Basáñez, G., Nieva, J.-L., Goñi, F. M., and Alonso, A. (1996) Origin of the lag period in the phospholipase C cleavage of phospholipids in membranes. Concomitant vesicle aggregation and enzyme activation, *Biochemistry 35*, 15183−15187.
43. Zasloff, M. (2002) Antimicrobial peptides of multicellular organisms, *Nature 415*, 389−395.
44. Baker, B. Y., Yaworsky, D. C., and Miller, W. L. (2005) A pH-dependent molten globule transition is required for acitivity of the steroidogenic acute regulatory protein, StAR, *J. Biol. Chem. 280*, 41753−41760.
45. Song, M., Shao, H., Mujeeb, A., James, T. L., and Miller, W. L. (2001) Molten-globule structure and membrane binding of the N-terminal protease-resistant domain (63−193.) of the steroidogenic acute regulatory protein (StAR), *Biochem. J. 356*, 151−158.
46. Yaworsky, D. C., Baker, B. Y., Bose, H. S., Best, K. B., Jensen, L. B., Bell, J. D., Baldwin, M. A., and Miller, W. L. (2005) pH-dependent Interactions of the carboxy-terminal helix of steroidogenic acute regulatory protein with synthetic membranes, *J. Biol. Chem. 280*, 2045−2054.

BI062058H